Syntheses, Structures, and Preliminary Electrochemistry of the Layered Lithium and Sodium Manganese(IV) Oxides, $A_2Mn_3O_7$

E. A. Raekelboom, A. L. Hector, J. Owen, G. Vitins, and M. T. Weller*

Department of Chemistry, University of Southampton, Southampton, SO17 1BJ, United Kingdom

Received April 12, 2001. Revised Manuscript Received August 13, 2001

$Li_2Mn_3O_7$ (Mn(IV)) has been obtained, by ion exchange in nonaqueous media, from $Na_2Mn_3O_7$ prepared at high pressure. The structures of both materials have been investigated by powder neutron diffraction. $Na_2Mn_3O_7$ has been found to adopt the structure previously described in the literature, but evidence of stacking disorder of the $Mn_3O_7^{2-}$ layers is observed. The structure of $Li_2Mn_3O_7$ is based on the same manganese deficient MnO_2 layers of stoichiometry $Mn_3O_7^{2-}$ but with an arrangement similar to that found in α-$NaFeO_2$ with lithium disordered over partially occupied octahedral sites between the layers. Preliminary investigations of the electrochemical properties of $Li_2Mn_3O_7$ reveal a good capacity of 160 mAh g^{-1} and retention of the capacity over at least 30 cycles.

Introduction

Complex oxides of the first-row transition metals with lithium have been the subject of considerable recent interest due to their potential application as cathodes in secondary lithium batteries. Compounds investigated include those of vanadium, manganese, iron, cobalt, nickel, and copper in materials such as $Li_xV_2O_5$,[1] $LiMn_2O_4$[2], $LiCoO_2$[3], $LiNiO_2$[3], and $Li_3Cu_2O_4$.[4] Of these systems, particular attention has been directed at the complex oxides of cobalt and manganese as these form the basis of commercial rechargeable lithium ion batteries.

The lithium cobalt oxide system contains the two main phases: rhombohedral $LiCoO_2$ and cubic $Li_{1-x}Co_xO$.[5] Two further phases, Li_4CoO_4[6] and $Li_{57}Co_{19}O_{48}$[7], have also been described. The lithium manganese oxide system is rather more complex with a number of phases obtainable either by direct reaction or via chimie douce methods. $LiMnO_2$ (Mn(III)) exists under four polymorph phases: orthorhombic,[8] monoclinic[9] (see below), low-temperature tetragonal,[10] and high-temperature tetragonal.[11] The structures of the various $LiMnO_2$ polymorphs are influenced by Jahn−Teller distortion of the Mn−O octahedron, reducing the local manganese symmetry. For this reason, there is no directly obtainable structural analogue of hexagonal $LiCoO_2$ among the $AMnO_2$ (A = alkali metal) compounds. Spinel-type compounds in the lithium manganese oxide system include $Li_2Mn_4O_9$ and $Li_4Mn_5O_{12}$ with Mn(IV). These compounds can be used in the 3 V lithium rechargeable cells. $Li_xMn_2O_4$ ($x = 1.00, 1.04, 1.03$) offer a high potential of 4 V but suffer from bad capacity retention.[12] Phases based on Li_2MnO_3 are discussed in detail below.

In terms of battery applications, the cobalt system $Li_{1-x}CoO_2$ has advantages associated with its sheetlike structure which allows lithium ions to be extracted from between the layers with little structural rearrangement. However, the cost and toxicity problems associated with cobalt have led to recent attention being directed at systems containing cheaper, low-toxicity metals such as manganese and iron. Bruce et al.[9] have managed to induce similar structural features of those of $Li_{1-x}CoO_2$ into manganese oxides with the formation of layered $LiMnO_2$ from α-$NaMnO_2$ through a low-temperature ion-exchange reaction. Lithium may be extracted from this system to produce $Li_{1-x}MnO_2$ ($0 < x < 1$). However, with manganese, the formation of a Mn^{3+} d^4 system and the cycling through this oxidation state during intercalation−deintercalation result in structural instabilities resulting from the formation−destruction of the Jahn−Teller ion. These maybe overcome to some extent through partial replacement of manganese by cobalt in the same structure, $LiMn_{1-x}Co_xO_2$. However, this defeats to a large degree the purpose of developing cobalt

(1) Day, A. N.; Sullivan, B. P. U.S. Patent 3, 1972, *655*, 585.
(2) Ohzuku, T.; Kitagawa, M.; Hirai, T. *J. Electrochem. Soc.* **1990**, *137*, 769.
(3) (a) Plichta, E.; Salomon, M.; Slane, S.; Uchiyama, M.; Chua, D.; Ebner, W. B.; Lin, H. W. *J. Power Sources* **1987**, *21*, 25. (b) Thomas, M. G. S. R.; David, W. I. F.; Goodenough, J. B.; Groves, P. *Mater. Res. Bull.* **1985**, *20*, 1137.
(4) Raekelboom, E. A.; Hector, A. L.; Weller, M. T.; Owen, J. R. Accepted for publication in *J. Power Sources*.
(5) Johnston, W. D.; Heikes, R. R.; Sestrich, D. *J. Phys. Chem. Solids* **1958**, *7*, 1.
(6) Jansen, M.; Hoppe, R. *Naturwissenschaften* **1973**, *60*, 104.
(7) Jansen, M.; Kastner, P.; Hoppe, R. *Z. Anorg. Allg. Chem.* **1975**, *414*, 69.
(8) Hoppe, R.; Brachtel, G.; Jansen, M. *Z. Anorg. Allg. Chem.* **1975**, *417*, 1.
(9) Armstrong A. R.; Bruce, P. G. *Nature* **1996**, *381*, 499.
(10) Thackeray, M. M.; David, W. I. F.; Bruce, P. G.; Goodenough, J. B. *Mater. Res. Bull.* **1993**, *18*, 461.
(11) Reimers, J. N.; Falkner, T.; Bonakdarpour A. B. In *Abstract in the Electrochemical Society Meeting*, Chicago, Oct 8−13, 1995; *95-2*, No. 90.
(12) Tarascon, J. M.; Wang, E.; Shokoohi, F. K.; McKinnon, W. R.; Colson, S. *J. Electrochem. Soc.* **1991**, *138*, 2859.

10.1021/cm011105j CCC: $20.00
Published on Web 10/09/2001

free batteries due to the perceived toxicity and costs associated with this element. Two more points are of further concern regarding the performance of $LiMnO_2$-based systems. First, the high oxidation states involved in the $Li_{1-x}CoO_2$ (Co(III/IV)) system produce desirable, higher voltages than the Mn(III/IV) cycle. Second, the $LiMnO_2$ system is somewhat limited in terms of discharge range since only half the quantity of lithium can be reinserted from the first cycle.

A desirable goal is therefore a new lithium ion system based on Mn(IV) rather than Mn(III), as potential advantages associated with the low toxicity of manganese might be coupled with avoidance of high levels of Mn(III) during cycling, higher cell potential, and a greater discharge range. The alkali metal−manganese oxide systems contain a number of high oxidation state manganese compounds based on discrete ions, for example, lithium manganate(IV) (Li_2MnO_4) and hypermanganates (Mn(V)). However, the presence of discrete MnO_4^{n-} ($n = 1, 2, 3$) species in these materials and their highly oxidizing and reactive natures lead to them being unsuitable for rechargeable battery systems where a more rugged, linked structure is desirable. Only a few pure Mn(IV) alkali metal oxides have been synthesized directly rather than through electrochemical oxidation/extraction methods. One of these, $Na_2Mn_3O_7$, reported by Chang and Jansen[13] has a layered structure based on $Mn_3O_7^{2-}$ layers formed from linked MnO_6 octahedra separated by sodium ions, Figure 1. The structure may be viewed as a layer of edge-linked MnO_6 octahedra, as in the $NaFeO_2$ structure type, but with one-seventh of the transition metal ions removed in a regular manner from the layer. The structure of this material was determined from a single crystal, and no work has been carried out on bulk compound since then.

The structure of Li_2MnO_3 (Mn(IV)) can be considered as layered in terms of filling of the octahedral holes in a close-packed array of oxide ions; the cations form sheets with lithium layers alternating with those of mixed lithium (33%) and manganese (67%). The electrochemical behaviors of this material and its delithiated derivatives have been investigated,[14,15] and the characteristics are similar to those of other rocksalt or spinel derived structures, with the same limitations.

In this paper, we report the bulk synthesis of $Na_2Mn_3O_7$ and a derivative, $Li_2Mn_3O_7$, formed through a low-temperature, ion-exchange route. The layered structures of both materials have been refined from powder neutron diffraction data. We also report preliminary findings on the electrochemical behavior of $Li_2Mn_3O_7$.

Experimental Section

$Na_2Mn_3O_7$ was prepared hydrothermally from the required stoichiometric mixture of oxides MnO_2 and Na_2O by heating at 600 °C under 1.4 kbar for 2 days.[13] The product was ground in the glovebox (MBraun Labmaster130, <1 ppm O_2 and H_2O) to a dark gray powder. Phase purity was verified by powder X-ray diffraction using a Siemens D5000 diffractometer operating in reflection mode with Cu $K\alpha_1$ radiation.

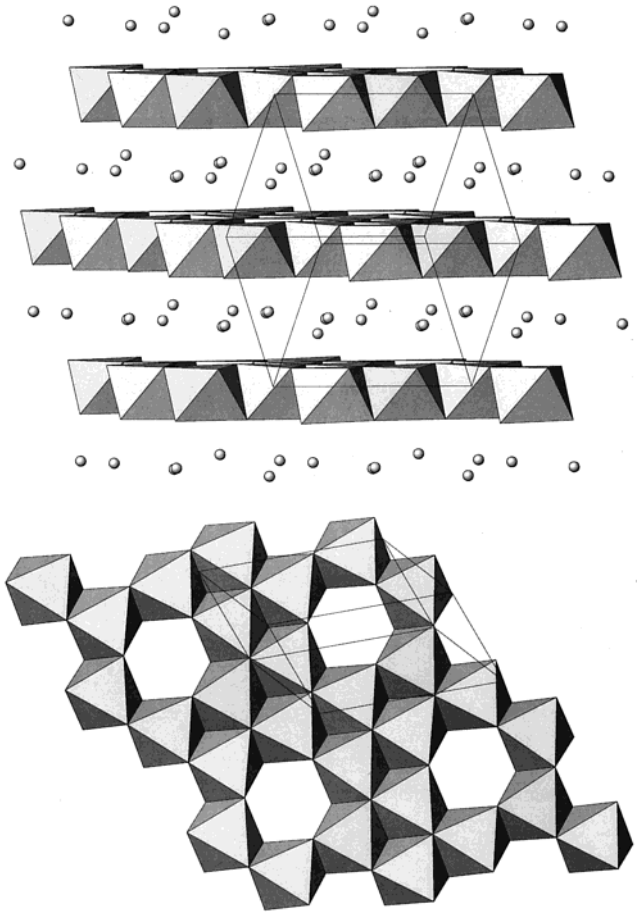

Figure 1. Structure of $Na_2Mn_3O_7$ viewed as follows: (a) close to parallel to the layers and (b) perpendicular to a single $Mn_3O_7^{2-}$ layer; MnO_6 octahedra are shown, sodium atoms are shown as shaded spheres.

The synthesis of $Li_2Mn_3O_7$ was achieved through a chemie douce type replacement of the sodium in $Na_2Mn_3O_7$ by lithium. The ion-exchange reaction involved refluxing, under nitrogen, the sodium phase in dry distilled ethanol at 70 °C with a 20-fold excess of dry LiBr (Aldrich) and a 6-fold excess of 15-crown-5 ether (Aldrich), to facilitate the extraction of sodium into the solution, for 12 h. After the mixture was cooled, the solid product was recovered, washed with dry ethanol, and dried under vacuum.

Lithium content of the product was determined by flame emission analysis on a Corning 400 flame photometer, and the manganese concentration was determined photometrically by UV−visible spectroscopy (Perkin-Elmer Lambda19) after dissolution of the compound in concentrated sulfuric acid (0.5 mL) and potassium periodate (saturated solution of KIO_4). The manganese oxidation state was determined by titration with ferrous sulfate solution.[16] Scanning electron microscopy (SEM) was carried out on a JEOL 6400 to investigate the morphology of the lithiated product.

Both the parent phase, $Na_2Mn_3O_7$, and the ion-exchange product were further characterized using neutron diffraction. Time-of-flight powder neutron diffraction data were collected on the POLARIS ($Li_2Mn_3O_7$) and HRPD ($Na_2Mn_3O_7$) instruments at ISIS, Rutherford Appleton Laboratory. The structures were refined by the Rietveld method using the GSAS package.[17]

Electrodes were prepared by forming a composite between the $Li_2Mn_3O_7$ cathode material, Cabot carbon black, and poly-

(13) Chang, F.; Jansen, M. *Z. Anorg. Allg. Chem.* **1985**, *531*, 177.
(14) Roussouw M. H.; Thackeray, M. M. *Mater. Res. Bull.* **1991**, *26*, 463.
(15) Johnson, C. S.; Korte, S. D.; Vaughey, J. T.; Thackeray, M. M.; Bofinger, T. E.; Shao-Horn, Y.; Hackney, S. A. *J. Power Sources* **1999**, *82*, 491.
(16) Katz, M. J.; Clarke, R. C.; Nye, W. F. *Anal. Chem.* **1956**, *28*, 507.
(17) von Dreele, R. B.; Larson, A. C. *Generalised Structure Analysis System*; Los Alamos, NM, 1998.

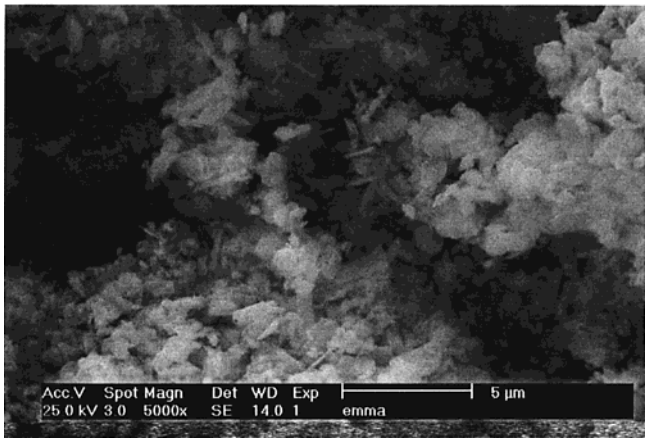

Figure 2. SEM image of $Li_2Mn_3O_7$ showing plates of dimension 1 μm.

(tetrafluoroethylene) binder in the weight ratios of 60:30:10. Electrodes were pressed and rolled using (Durston) mini rolling mills. Pellets were cut (diameter = 10 mm, thickness = 100 μm) and dried under vacuum at 100 °C for 1 day. A stainless steel cell was used for constant current cycling on the composite insertion electrode. The electrolyte consisted of a 1 M solution of $LiPF_6$ dissolved in 1:1 EC/DMC. A glass filter (Whatman) was used as separator, and lithium metal was used as the anode. A custom-built computer battery charge−discharge testing unit was used for galvanostatic cycling.

Results

Analysis of $Li_2Mn_3O_7$. Atomic emission analysis was used to determine the lithium content following calibration of the apparatus using standard solutions of lithium. A lithium percentage of 3.3 ± 0.5% was determined, compared with a value of 4.7% expected for an idealized product stoichiometry of $Li_2Mn_3O_7$. Analysis for sodium was also undertaken, and only a very small level of residual sodium was found in the compound (<0.5%). UV−vis spectrophotometric analysis for manganese gave 47.5% of Mn, compared with 55.4% expected for $Li_2Mn_3O_7$. Further confirmation of the product stoichiometry was obtained from the titration according to the ferrous ammonium sulfate method,[16] which gave a manganese oxidation state of 3.95 ± 0.1 demonstrating that no change in oxidation state occurred during the ion-exchange process. Overall, the analysis results are in good agreement with the exchange of sodium by lithium and the results obtained from the structure analysis, vide infra. The slight, but significant, deficiency of lithium can be attributed to a number of factors such as a small amount of residual sodium or a low level of lithium (oxide) leaching from the compound during the ion-exchange process, as can occur with materials such as Li_2MnO_3.

The SEM image of $Li_2Mn_3O_7$ (Figure 2) shows the presence of thin plates of 1 μm. This can be compared to the much larger crystallites of $Na_2Mn_3O_7$ that are grown under the hydrothermal conditions. A similar reduction in average crystallite dimension is observed in the powder X-ray diffraction patterns through the marked broadening of the reflections, Figure 3. This powder X-ray diffraction data also shows a marked shift in the position of the main reflection (from d = 5.57 to d = 4.8 Å), corresponding to the interlayer spacing, in agreement with the replacement of sodium by the smaller lithium ion between the layers.

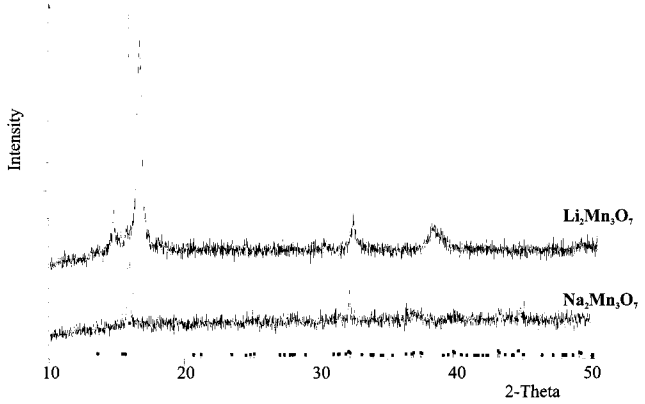

Figure 3. Powder X-ray diffraction patterns obtained from (i) $Na_2Mn_3O_7$ and (ii) $Li_2Mn_3O_7$; the stick pattern represents the calculated reflection intensities for $Na_2Mn_3O_7$.

Table 1. Refined Atomic Coordinates for $Na_2Mn_3O_7$[a]

atom	x	y	z	$Ui/Ue \times 100$ Å^2
Na1	0.252 000	0.690 900	0.491 200	1.36(18)
Na2	0.3351(25)	0.8264(22)	0.0695(28)	1.36(18)
Mn3	0.0568(25)	0.0922(23)	0.2316(27)	0.33(10)
Mn4	0.3223(22)	0.3582(20)	0.0731(28)	0.33(10)
Mn5	0.1995(28)	0.2169(27)	0.6455(28)	0.33(10)
O6	0.4060(18)	0.2185(17)	0.2695(20)	1.42(6)
O7	−0.2724(17)	−0.0560(16)	0.1729(20)	1.42(6)
O8	0.0380(19)	0.1972(18)	0.0273(20)	1.42(6)
O9	0.1467(17)	0.3526(16)	0.4564(20)	1.42(6)
O10	0.6829(19)	0.5294(18)	0.1275(19)	1.42(6)
O11	0.1080(16)	−0.0517(16)	0.4054(19)	1.42(6)
O12	0.4422(17)	0.6271(16)	0.3031(19)	1.42(6)

[a] Esds are given in parentheses. Space group $P\bar{1}$. Lattice constants: a = 6.619 09(14) Å, b = 6.839 62(10) Å, c = 7.5282(4) Å, α = 105.7735(22)°, β = 106.8409(28)°, γ = 111.6316(13)°. Cell volume = 274.400(17) Å^3.

Structure Refinement of $Na_2Mn_3O_7$. The structure of $Na_2Mn_3O_7$ reported by Chang and Jansen[13] was obtained from a single-crystal X-ray diffraction study. This structure refinement was carried out on a tabular crystal, and despite the low symmetry, only 1000 reflections were used in the refinement producing a fit factor of over 6%. This structural model, despite some concerns over its quality, was used as the basis for the refinement. All peaks in the diffraction profile could be indexed using the triclinic unit cell given previously[13] though the majority of the reflections were very weak. Attempts to re-index the data using a simpler or higher symmetry unit cell were unsuccessful. Refinement was undertaken using the normal stages of profile refinement involving gradual introduction of profile parameters, atomic positions, and temperature factors. The refinement converged to give the positional parameters summarized in Table 1 and the profile fit shown in Figure 4. Inspection of this profile fit and the values obtained for R_{wp} and R_p of 11.58 and 9.27%, respectively, indicates that this structural model is not ideal. The main deficiencies in the profile fit were investigated and determined as being derived from a number of reflections whose Miller indices corresponded to the planes representing directions perpendicular to the manganese−oxygen layers, e.g., (3,−3,0). Attempts to overcome these problems using a variety of preferred orientation parameters and anisotropic peak-broadening terms were only partially successful. In conclusion, the basic structural model seems correct, producing a reasonable

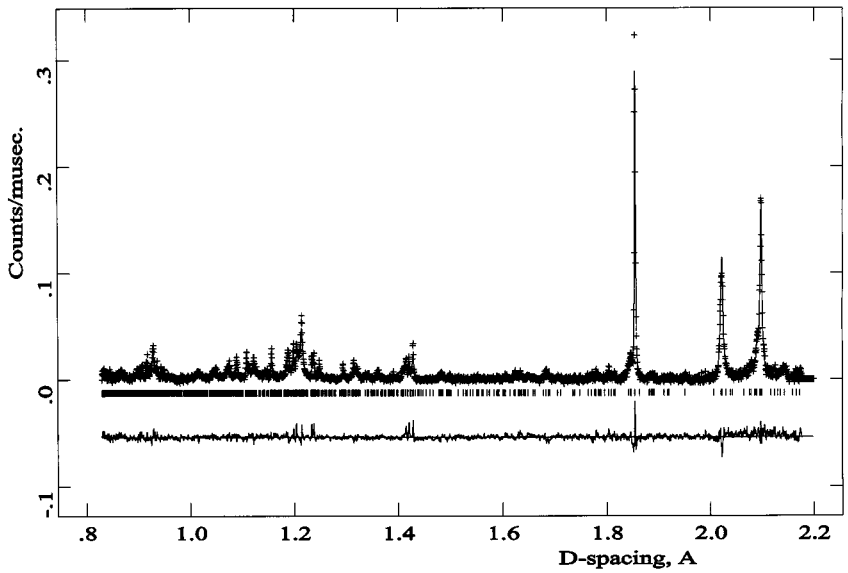

Figure 4. Final profile fit obtained to the powder neutron diffraction data obtained from $Na_2Mn_3O_7$; cross marks show experimental data, the upper continuous line shows the calculated profile and the lower continuous line shows the difference and tick marks show reflection positions.

profile fit and full indexing of the data, but the true structure of this material in polycrystalline form is obviously more complex. One possibility is that in the bulk, powdered form, $Na_2Mn_3O_7$ loses the stacking sequence of the crystallographic description, that is, the $Mn_3O_7^{2-}$ layers are no longer perfectly aligned throughout the crystal structure; such behavior is common in materials with layered structures. This behavior is also supported by the powder X-ray diffraction patterns obtained from $Na_2Mn_3O_7$ (see Figure 3); only one peak composed of the (−110) + (100) reflections is observed with any intensity. This reflection corresponds to scattering from the $Mn_3O_7^{2-}$ planes separated by a distance of 5.57 Å but does not rely on registration of the planes throughout the structure.

Structure Refinement of $Li_2Mn_3O_7$. Inspection of the diffraction pattern obtained from $Li_2Mn_3O_7$ showed that the reflections could be indexed on a simple hexagonal unit cell of dimensions: $a = 2.8 \times c = 14.5$ Å, similar to that adopted by layered oxides of the stoichiometry AMO_2. The peak widths were markedly increased in comparison with the parent phase indicating a further degradation of the three-dimension order following ion exchange (Figure 3). Refinement of the structure was therefore considered in the variety of structure models that have been used to represent AMO_2 layer structures such as the monoclinic layered $C2m$, cubic spinel $Fd\bar{3}m$, and orthorhombic $Pmmn$, but the best fit was found for the $R\bar{3}m$ space group of α-$NaFeO_2$.

The atomic positions of α-$NaFeO_2$ were used to describe the structure of $Li_2Mn_3O_7$, with the lithium and manganese ions located on the 3b and 3a sites, respectively. Initial stages of the refinement involved the profile factors and the one refineable positional parameter. In the later stages of the refinement, the occupancies of the various sites were permitted to vary without constraint. Convergence was achieved, and the final profile fit parameters obtained for the compound were good; crystallographic data obtained are summarized in Table 2. Given the disordered structure type and reflection widths, the final profile fit achieved, Figure 5, was excellent. Figure 6 shows the average $Li_2Mn_3O_7$ structure with manganese deficient sheets formed from disordered edge-sharing MnO_6 and $\square O_6$ octahedra (where □ represents a manganese vacancy) separated by sheets of approximately octahedrally coordinated lithium ions.

Table 2. Refined Atomic Coordinates for $Li_2Mn_3O_7$[a]

atom	site	occupancy	*x*	*y*	*z*	*Ui*/*Ue* × 100 Å^2
Li	3a	0.48(10)	0	0	0.5	6.0(23)
Mn	3b	0.890(23)	0	0	0	0.38(8)
O	6c	1	0	0	0.264 60(15)	0.78(4)

[a] Esds are given in parentheses. Space group: $R3m$. a = 2.839 61(11) Å, c = 14.486(5) Å, R_{wp} = 2.98%, R_p = 4.69%, χ^2 = 5.541.

The refined lithium and manganese occupancies were found to be significantly less than unity refining to values of 0.48(10) and 0.890(23), respectively. These values represent partial filling of the octahedral sites, both between and within the "MnO_2" layers, and are in good agreement with values obtained from chemical analysis. Rewriting the crystallographically determined stoichiometry of $Li_{0.48}[Mn_{0.89}O_2]$ in terms of the same oxygen sheet stoichiometry as of $Na_2Mn_3O_7$ gives the formula $Li_{1.7}Mn_{3.1}O_7$. That is, the manganese deficiency in the octahedral layers is maintained at the level of the sodium parent phase and the alkali metal stoichiometry of the octahedral sites between the layers is also similar. The only difference between the structures is that there is an increased disorder of the cations between the layers and the positions of the manganese ion vacancies in neighboring sheets also lose their fixed relative positions. That is, the Mn_3O_7 layers remain in the ion-exchanged compound, presumably, with the same distribution of the one-seventh of the Mn vacancies as exists in $Na_2Mn_3O_7$, Figure 1, but the ion-exchange reaction causes a complete disordering of these sheets along the *c* direction of $Li_2Mn_3O_7$.

Consideration of the manganese environment in $Li_3Mn_2O_7$ shows this to be a slightly trigonally distorted octahedron with the Mn−O bond length of (×6) 1.913 Å and the O−Mn−O bond angle of 84.6°. This geometry

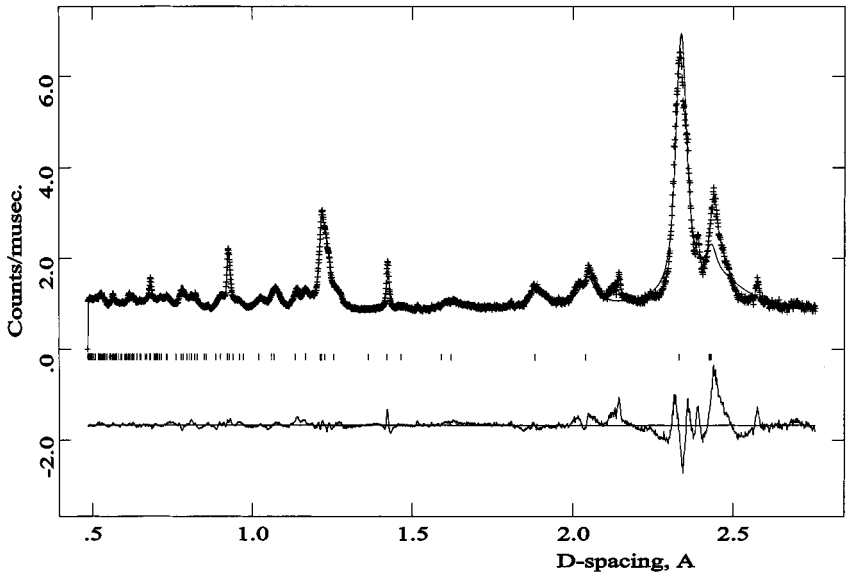

Figure 5. Final profile fit obtained to the powder neutron diffraction data obtained from $Li_2Mn_3O_7$; cross marks show experimental data, the upper continuous line shows the calculated profile and the lower continuous line shows the difference and tick marks show reflection positions. The peak at 2.14 Å is due to the vanadium sample can.

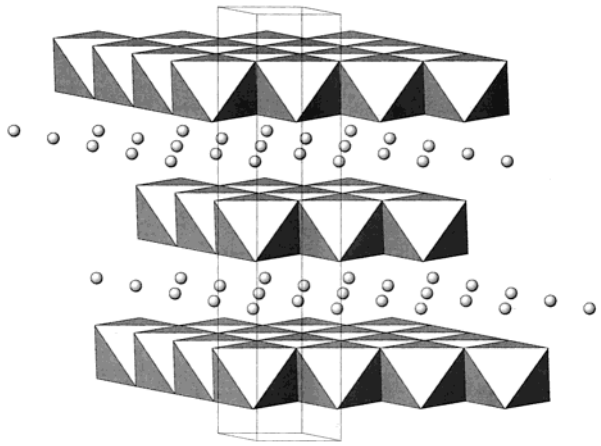

Figure 6. Structure of $Li_2Mn_3O_7$; manganese deficient MnO_6 octahedra are shown as the partially occupied lithium sites (shaded spheres).

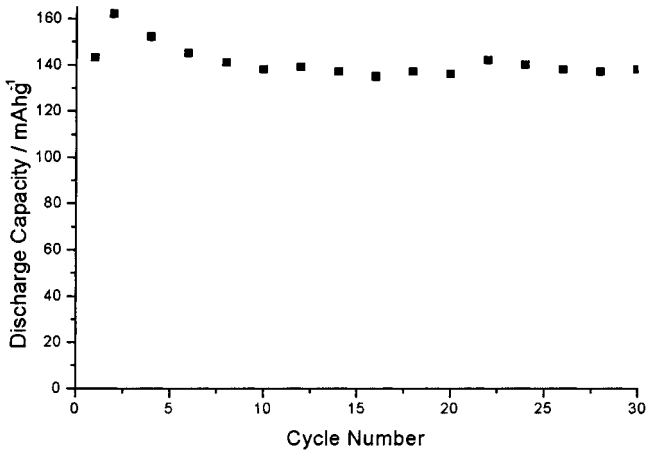

Figure 7. Discharge capacity of the layered $Li_2Mn_3O_7$ as a function of cycle number between 2 and 4.5 V.

is typical of Mn(IV) and quite different from that of the Jahn−Teller distorted Mn(III). In the case of $LiMnO_2$, the localized high-spin $3d^4$ ($t_{2g}^3e_g^1$) configuration of the Mn^{3+} ion induces a cooperative Jahn−Teller distortion of the octahedral sites lowering the crystal symmetry from rhombohedral ($R3m$) to monoclinic ($C2/m$) with Mn−O bond lengths of 1.92 Å × 4 and 2.31 Å × 2. In $Li_2Mn_3O_7$, the high oxidation state of manganese (3.95 (d^3)) is not Jahn−Teller active and a single undistorted phase of rhombohedral symmetry is obtained. The lithium ions also adopt distorted octahedral sites with Li−O = 2.16 Å which is typical for this ion in this coordination geometry.

The Electrochemistry of $Li_2Mn_3O_7$: Preliminary Results. The cycling was carried out at a current density of 0.6 mA cm^{-2}. The charge and discharge curves are shown in Figure 7. The material was first discharged from its OCV of 3.28 to 2 V offering a capacity of 140 mAh g^{-1} corresponding to 0.48 lithium ions per formula unit intercalated to $Li_2Mn_3O_7$ on initial discharge. The cycling was subsequently carried out between 2 and 4.5 V. During the first charge, the material develops a plateau in the 3 V region with a discharge capacity of 160 mAh g^{-1} corresponding to the de-intercalation of the lithium ion from the interlayer octahedral sites. After several cycles, the discharge curves also exhibit the formation of a small plateau in the 4 V region which has been ascribed previously, in some other lithium−manganese systems where it is generally a very strong feature, to the formation of a spinel type structure.[9] Further investigations during cycling, which are in progress, will help to understand the reaction in this region. Although evidence of a structural change in part of the material is apparent, the discharge capacity is quite stable over this range after 30 cycles (Figure 8). After the initial rise within the first 3 cycles, the capacity varies little with cycle number.

Incremental capacity plots of $Li_2Mn_3O_7$ are shown (Figure 9). It is apparent that the peaks in the 4 V region appear only during the initial charge of $Li_2Mn_3O_7$. This is accompanied by a gradual decrease of the oxidation peak at 3 V; a reduction process at 3.9 V appears weakly after 5−10 cycles and more strongly by 20−30 cycles.

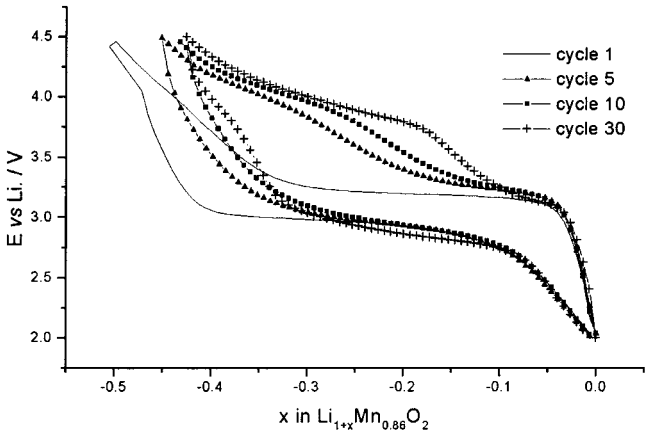

Figure 8. Charge and discharge curves collected at a constant current of 0.6 mA cm^{-2}. The *x*-axis gives the number of lithium ions per formula de-intercalated in the layered $Li_{0.96}Mn_{0.89}O_2$ after the initial discharge.

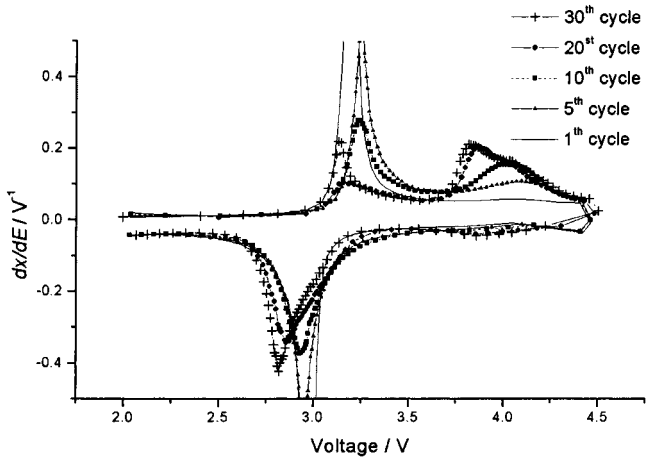

Figure 9. Incremental capacity plot of $Li_2Mn_3O_7$ cycled at 0.6 mA cm^{-2} up to 30 cycles.

Formation of the spinel phase has been already reported for *o*-$LiMnO_2$,[18] monoclinic $LiMnO_2$,[19] and the layered cobalt-substituted $LiMn_{1-x}Co_xO_2$.[20] A strong additional plateau at 3.8 V was always noticed after few cycles (<5). Also, a greater stability of the layered structure of $LiMnO_2$ has already been reported when cobalt is substituted for manganese, $LiMn_{1-x}Co_xO_2$ ($0.1 < x < 0.3$). The transformation into spinel was found to be slower only with a high cobalt content (>30%).[20] The data presented here indicate that the cobalt-free layered $Li_2Mn_3O_7$ can be stable during the initial cycling showing only a weak peak at 3.9 V even after 5−10 cycles; this feature was considered as possibly arising from the formation of a spinel type structure. However, powder X-ray diffraction data collected on cell material which had been cycled 30 times showed no evidence of a spinel phase with just a small shift, to smaller d spacings, in the main reflection positions. A more likely explanation of this feature is the gradual formation of a small amount of an intermediate structure type on lithium intercalation, where lithium enters the manganese layers either into the vacant sites in the Mn_3O_7 layers or by kicking manganese out to interlayer sites formerly occupied by lithium.

As with the Co-doped phase, this stability of $Li_2Mn_3O_7$ can be associated with the mitigation of strong Jahn−Teller distortion effects during the cycling of this new layered Mn(IV) based phase. That is, the initial discharge to effectively give $LiMn_{0.86}O_2$ produces at most 50% of Mn(III) in the structure and any Jahn−Teller effects, such as structural distortions, are reduced in influence. Further, even if an intermediate type structure is being formed on cycling, then this material is likely to have a high level of defects, for example, due to the manganese deficiency in octahedral sites of the parent phase, which might improve cell characteristics.

Conclusion

The sodium ions in the layered manganate $Na_3Mn_2O_7$ can be ion exchanged in nonaqueous condition to yield a new lithium manganese(IV) complex oxide. The basic layer structure with $Mn_3O_7^{2-}$ is maintained during this process, but increased disorder between the individual oxide layers is induced. The product phase $Li_2Mn_3O_7$ has the ideal structural and chemical characteristics of a cathode for rechargeable lithium ion batteries with sheets of lithium sandwiched between Mn(IV) oxide layers. The system may be discharged in a lithium ion cell without generating a high level of Mn(III), which would result in massive disruption of the structure. Initial investigations of the cell characteristics of $Li_2Mn_3O_7$ show good capacity, reasonable cell voltages, and retention of cell capacity on cycling. Further investigations of the electrochemical characteristics of this material are in progress.

Acknowledgment. We thank the EPSRC for support under Grant No. GR/M03610.

CM011105J

(18) (a) Reimers, J. N.; Fuller, E. W.; Dahn, J. R. *J. Electrochem. Soc.* **1993**, *140*, 3396. (b) Gummow, R. J.; Thackery M. M. *J. Electrochem. Soc.* **1994**, *141*, 1178.

(19) Tabuchi, M.; Ado, K.; Kobayashi, H.; Kageyama, H.; Masquelier, C.; Kondo, A.; Kanno, R. *J. Electrochem. Soc.* **1998**, *145*, L49.

(20) Armstrong, A. R.; Robertson, A. D.; Gitzendanner, R.; Bruce, P. *J. Solid State Chem.* **1999**, *145*, 549.